Photoelectric characteristics and surface morphology of cadmium sulfide modified by iron arachinate

© P.G. Kharitonova, E.G. Glukhovskoy, A.V. Kozlowski, S.V. Stetsyura

Saratov National Research State University,
410012 Saratov, Russia

E-mail: haritonovapg@gmail.com

The influence of the nanoscale coating of iron arachinate (ArchFe) on the properties of CdS has been studied. We obtained changes in the morphology and potential of the surface, as well as in the photosensitivity of the CdS/ArchFe hybrid structure compared to unmodified CdS. We have shown the possibility of creating a heterophase structure with photosensitivity and properties of a semimagnetic semiconductor after annealing, which leads to sublimation of the organic component of the coating and diffusion of Fe deep into CdS, accompanied by the formation of nanosized FeS inclusions.

Keywords: cadmium and iron sulfides, Langmuir–Blodgett technology, surface modification, photoelectric properties.

Currently, much attention is being paid to the creation of new materials that have enhanced functionality. Modification of previously known materials allows their properties to be modified, which can be controlled by various external influences [1]. In this aspect, a promising material is cadmium sulfide (CdS), the alloying of which with metal atoms makes it possible to obtain structures with improved characteristics [2,3]. The possibility of creating heterophase magnetic sensitive structures based on polycrystalline CdS films by introducing Fe atoms into CdS was proved in our research [4]. As shown, Fe atoms diffuse from the metallized coating into the CdS film during the high temperature annealing process and form a solid solution $Cd_xFe_{1-x}S$. But due to the limited solubility of Fe in CdS, different rates of Fe diffusion within the crystallites and across the intergranular boundaries, several processes — precipitation, diffusion, and surface oxidation competed, leading to the formation of several kinds of phases unevenly arranged on the surface and in the volume. Thus, FeS and Fe_2O_3 phases were recorded, due to which the material exhibited the properties of a semi-magnetic semiconductor [4]. The study focused on the detection of magnetic properties, while the change in the photovoltaic characteristics of the CdS−FeS heterophase structure was not given due attention.

To establish the role of CdS polycrystalline structure and diffusion rate on the phase composition and functional properties of the final structure in this study, some of the experiments were carried out on CdS single-crystal wafers. In addition, the use of a single-crystal base is of independent interest, as research continues on single-crystals of cadmium chalcogenides to extend their range of applicability and improve the properties [5–7]. In this connection, special attention is paid to modifying the properties of the near-surface band of crystals. The aim of the present work is to obtain and investigate the iron arachinate layer $(Fe(Arch)_3)$ on a single-crystal CdS substrate as a dosed Fe source during the formation of the CdS−FeS heterophase structure.

For surface modification, the technique of ultrathin coating using the Langmuir−Blodgett [8] technique previously tested on polycrystalline films was used. The process regimes and conditions for the preparation of $Fe(Arch)_3$ films are described in detail in [9]. Monolayer transfer from the surface of the sub-phase containing $FeCl_3$ with a concentration of 10^{-3} mol/L to the substrate was carried out using the Langmuir − Schaeffer method. On based on the results of the pH sub-phase of the solution, 4.2 ± 0.05 was chosen to ensure the formation of the salt $Fe(Arch)_3$ without the formation of polynuclear hydro-complexes and Fe clusters in accordance with the data of [9,10]. The formation of the densely packed iron-containing layer was monitored by $\pi−A$ isotherms, according to which the value of the area per molecule A, in the densely packed phase is $0.22\,nm^2$ for the arachidic acid monolayer and $0.32\,nm^2$ for the iron-containing monolayer. It should be noted that the A value was maximum at the indicated pH value, indicating that almost all molecules of the arachidic acid monolayer reacted with Fe atoms to form $Fe(Arch)_3$. This allowed us to estimate the density of Fe atoms in the monolayer, which was $N_s = 3.125 \cdot 10^{14}\,cm^{-2}$. The number of transferred monolayers was increased to 25 to increase the specific concentration of Fe atoms in the organic coating.

The quality of the $Fe(Arch)_3$ coating was determined by atomic-force microscopy (AFM) on a „NTEGRA-Spectra" (NT-MDT probe station, Russia). Scanning was performed in semi-contact mode using a platinum-coated FMG01/Pt cantilever and the resolution was 512×512 dots. Data
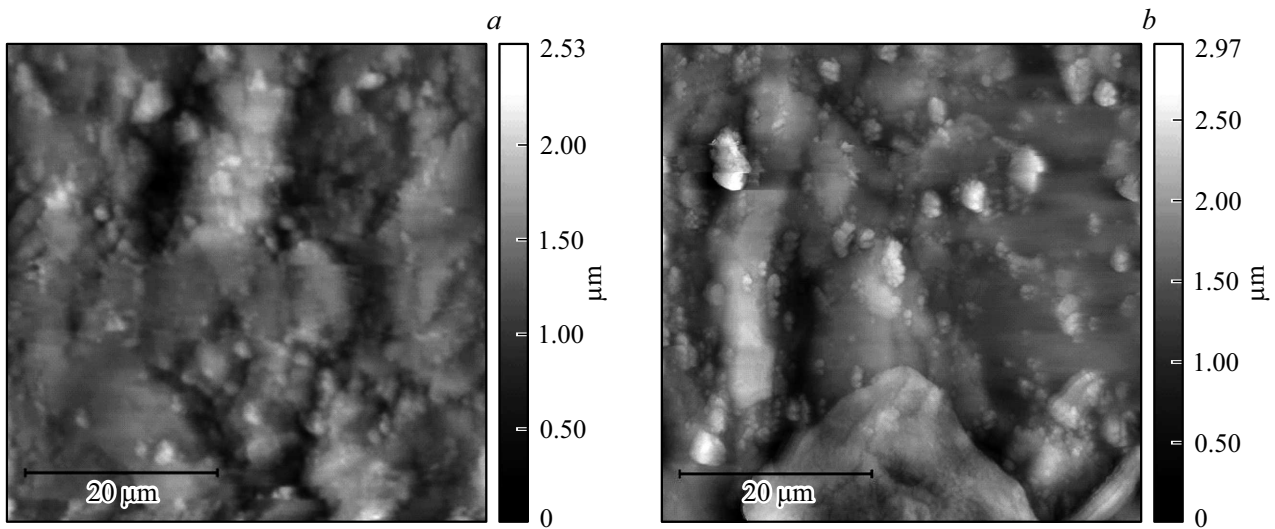
Figure 1. AFM images of uncoated CdS (*a*) and CdS/Fe(Arch)$_3$ (*b*) surfaces.

processing was performed using Gwyddion 2.62 software. A comparison of the surface topography of CdS with and without iron arachinate coating is presented in Figure 1.

The surface of the CdS single-crystal exhibits roughness at the submicron level, which allowed us to study the intrinsic morphology of the coating Fe(Arch)$_3$. According to AFM data, after application of the film Fe(Arch)$_3$, the average roughness of Sa increased from 231.1 to 260.6 nm (by 13%), and the RMS roughness of S_q increased from 297.7 to 331.1 nm (by 11%), which indicates that the layer Fe(Arch)$_3$ is sufficiently homogeneous in thickness and evenly distributed on the substrate during application.

Scanning Kelvin probe microscopy (SKPM) studies showed that the average value of the surface potential φ for uncoated CdS is 0.74 ± 0.04 V. After the application of Fe(Arch)$_3$, the value of φ increased to 2.10 ± 0.51 V. Thus, the average value φ increased by 180%. The distribution of φ over the uncoated CdS surface is fairly uniform — the scatter does not exceed 5%. Application of Fe(Arch)$_3$ against the background of a general increase φ leads to its drops of up to 24%, which is due to the presence of metal atoms in the poorly conductive organic coating.

In order to investigate the effect of the Fe(Arch)$_3$ coating on the photovoltaic characteristics of CdS, the current-voltage curve (CVC) of the investigated structures were measured in the dark and under illumination. CVC was measured on a PM-5 Cascade Microtech probe station using an Agilent B1500A analyzer. A Motic MLK-150C halogen lamp with an illumination intensity of 20000 lx in the sample plane was used for illumination. CVCs in the transverse mode of photoconductivity provide information about changes in the electrical properties of near-surface bands, which is important in modifying surface properties. The distance between the contacts was kept constant at $800\,\mu$m. The measurement and equivalent schemes illustrating the transverse photoconductivity mode and current

flow features in the hybrid structure, and the current-voltage curves measured in the dark and under illumination are shown in Figure 2.

As can be seen from Figure 2, the character of current variation under illumination and in the dark does not change when Fe(Arch)$_3$ coating is applied. The presence of the coating decreases the current both in the dark and under illumination, and the dark resistance of CdS/Fe(Arch)$_3$ increased 2.5 times, and the current at the specified illumination decreased only 1.3 times in comparison with the CdS sample, i.e., the multiplicity of change in the light resistance of the hybrid structure CdS/Fe(Arch)$_3$ remained at the same level. Since Fe(Arch)$_3$ is not sensitive to wavelengths from the halogen lamp spectrum, and the CdS/Fe(Arch)$_3$ hybrid structure retains photosensitivity, this means that current flows not only through the iron-structured organic film, but also through the CdS near-surface layer, while overcoming the resistance of the film Fe(Arch)$_3$ along its nanoscale thickness (Figure 2, a).

The next stage of surface modification consisted in annealing in air of the obtained structure at $500°$C for 30, 40 and 60 min. During the annealing process, the organic component of the coating sublimated, and Fe atoms diffused into CdS, changing the properties of its near-surface band. Also during annealing, there is a process of formation of precipitates, which begin to grow as soon as at a certain depth the concentration of Fe atoms exceeds the maximum permissible. Previously, it was experimentally shown that precipitation occurs with the formation of ferromagnetic phases FeS [4]. Investigation of the distribution of Fe atoms along the penetration depth in CdS by secondary ion mass spectrometry (SIMS) and the use of these data in the model of FeS precipitation in CdS allows us to determine the distribution of phases in the near-surface band of CdS. According to [8,11], in the case of formation of precipitates whose shape is close to spherical, the average
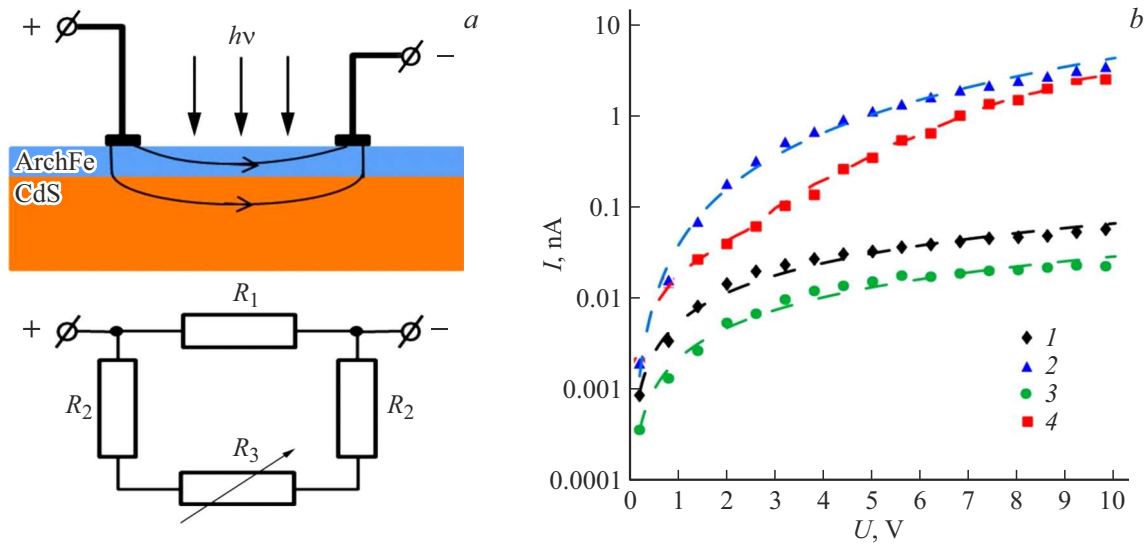
Figure 2. *a* — measurement and equivalent diagrams illustrating the transverse photoconductivity mode, where R_1 — resistance along the film Fe(Arch)$_3$, R_2 — resistance across the film Fe(Arch)$_3$, R_3 — photosensitive resistance of CdS; *b* — current-voltage curves of single-crystal CdS substrate (curves *1, 2*) and structure CdS/Fe(Arch)$_3$ (curves *3, 4*), measured in the dark (curves *1, 3*) and under illumination in the transverse photoconductivity mode (curves *2, 4*).
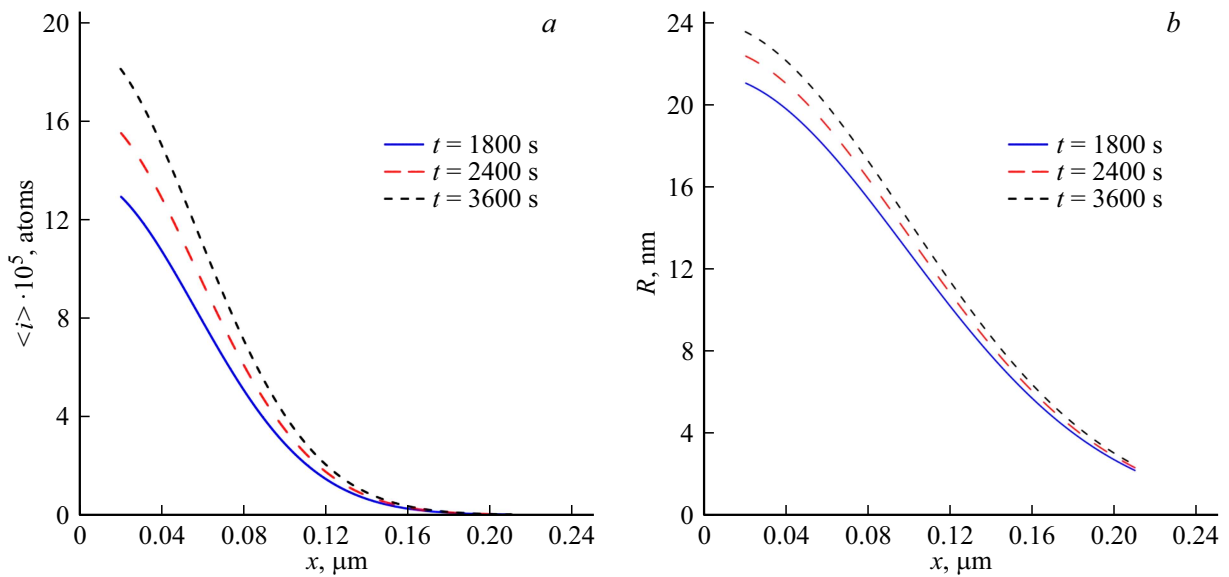

Figure 3. Dependence of the average number of particles in FeS precipitate (*a*) and the average radius of precipitate (*b*) on the depth of precipitates at different annealing times.

number of particles in the precipitate $\langle i \rangle$ and the radius of the precipitate R can be determined by the formulas:

$$\langle i(x,t) \rangle = \frac{1}{N_C} \int_0^t \frac{\partial N(x,t)}{\partial t}\, dt, \qquad (1)$$

$$R(t) = \left(\frac{3V_0 \langle i(x,t) \rangle}{4\pi} \right)^{1/3}, \qquad (2)$$

where $N(x,t)$ — the Fe concentration at a depth x from the surface resulting from diffusion of Fe atoms from a surface confined source with Fe concentration N_s, determined from the compression isotherms for Fe(Arch)$_3$, over an annealing time t. The dependencies $N(x,t)$ were determined experimentally from the SIMS profiles. The model previously presented in [8,11] was applied to determine the growth rate of $dN(x,t)/dt$ nanoclusters. The concentration of precipitate nucleation centers along the axis direction x N_C is assumed to be $8 \cdot 10^8\, \mu\mathrm{m}^{-1}$, the volume of one molecule FeS V_0 is $3.02 \cdot 10^{-2}\, \mathrm{nm}^3$. The calculated values of $\langle i \rangle$ and R for different annealing times are presented in Figure 3.

For the investigated material it is shown that FeS phases with radius more than 5 nm are formed at a depth up to 165 nm for 30 min of annealing, and at 60 min this depth is 175 nm. The maximum size of precipitates at the surface does not exceed 21 nm at $t = 30$ min and 24 nm at $t = 60$ min. Thus, prolonged annealing is not reasonable because it slightly increases $\langle i \rangle$ and R but oxidizes the CdS surface to a greater extent. As it was shown in [8], the obtained sizes and the distribution of nanoscale phases in depth are sufficient for the emergence of the material's new properties (in this case, semi-magnetic semiconductor), while the photosensitivity of CdS practically does not decrease, which increases the functionality of the material and controllability of its properties.

Funding

Conflict of interest

The authors declare that they have no conflict of interest.

References

[1] G.S. Khrypunov, A.V. Meriuts, T.N. Shelest, M.G. Khrypunov. Semiconductors, **53** (1), 89 (2019).
DOI: 10.1134/S1063782619010111

[2] S. Azam, Z. Abbas, Q. Bilal, M. Irfan, M.A. Khan, S.H. Naqib, R. Khenata, S. Muhammad, H. Algarni, A.G. Al-Sehemi, X. Wang. Physica B: Condensed Matter, **583**, 412056 (2020).
DOI:10.1016/j.physb.2020.412056

[3] B. Lohitha, S. Thanikaikarasan, S. Roji Marjorie. Materials Today: Proceedings, **33** (7), 3068 (2020).
DOI:10.1016/j.matpr.2020.03.513

[4] S.V. Stetsyura, P.G. Kharitonova, I.V. Malyar. Applied Physics, **5**, 66 (2020).
http://applphys.orion-ir.ru/appl-20/20-5/PF-20-5-66.pdf

[5] X.Q. Huo, H.Q. Si, K. Zhao, Y.W. Zhang, H.J. Cheng, Y.K. Xu. Journal of Semiconductors, **39** (12), 123003 (2018).
DOI:10.1088/1674-4926/39/12/123003

[6] S.U. Egarievwe, G. Yang, A.A. Egarievwe, I.O. Okwechime, J. Gray, Z.M. Hales, A. Hossain, G.S. Camarda, A.E. Bolotnikov, R.B. James. Nuclear Instruments and Methods in Physics Research A, **784**, 51 (2015).
DOI:10.1016/j.nima.2015.02.006

[7] K.A. Korolkova, A.V. Sel'kin, V.R. Novak. Physics of the Solid State, **61** (7), 1304 (2019).
DOI: 10.1134/S1063783419070175

[8] S.V. Stetsyura, E.G. Glukhovskoy, A.V. Kozlowski, I.V. Malyar, Technical Physics, **60** (5), 746 (2015).
DOI: 10.1134/S1063784215050266

[9] S.V. Stetsyura, P.G. Kharitonova, E.G. Glukhovskoy. St. Petersburg State Polytechnical University Journal. Physics and Mathematics, **15** (3.3), 250 (2022).
DOI: https://doi.org/10.18721/JPM.153.349

[10] A.I. Yanklovich. In *Uspekhi kolloidnoj khimii*, ed. by. A.I. Rusanova (Khimiya, Leningrad, 1991), p. 262-291. (in Russian)

[11] S.V. Bulyarskii, V.V. Svetukhin, O.V. Prikhod'ko. Semiconductors, **33** (11), 1157 (1999). DOI: 10.1134/1.1187839

Translated by Ego Translating